AUT Journal of Mechanical Engineering

AUT J. Mech. Eng., 6(4) (2022) 545-560
DOI: 10.22060/ajme.2022.20714.6015

Influencing Parameters on Tensile Modulus Characterization of Unidirectional Composite Laminates Using Digital Image Correlation Technique

A. Zarei Aziz, R. Sarfaraz*

Department of Mechanical and Energy Engineering, Shahid Beheshti University, Tehran, Iran

ABSTRACT: Digital image correlation as a well-established strain measurement technique is commonly employed for material characterization purposes. However, several parameters should usually be decided by users to attain accurate results with minimum processing time while there are few definite recommendations for the selection of these parameters. In the present study, the optimum setting of digital image correlation parameters is examined in order to minimize the processing time and sensitivity to the selection of parameters, and practical directions are advised to improve the efficiency of the technique. The performance of a typical analysis for the derivation of strain field and measurement of tensile modulus of a unidirectional carbon/epoxy composite laminate subjected to monotonic loading is experimentally assessed. The influence of setting parameters on the accuracy of measurement and the computational time required for the process is examined. The mutual influence of these parameters is also analyzed and discussed. Comparison of results shows the sensitivity of outputs to the selection of investigating parameters i.e. subset radius, subset spacing, and region of interest. The results show that an efficient gain from the maximum available region of digital images reduces the sensitivity of the analysis to these parameters. Moreover, the error introduced to the results is slightly increased by the increase of subset spacing while this influence can be diminished by enlarging the subset radius.

Review History:

Received: Oct. 27, 2021
Revised: Jul. 04, 2022
Accepted: Aug. 08, 2022
Available Online: Aug. 17, 2022

Keywords:

Digital image correlation
Subset size
Subset radius
Region of interest
Strain measurement.

1- Introduction

Digital Image Correlation (DIC) as a noncontact optical technique enables full-field surface strain measurement of an object by correlating the digital images taken during the loading of that object. This technique is increasingly being employed in various engineering applications thanks to its simple experimental setup and reasonably-priced equipment [1-4].

One of the potential applications of the DIC technique is in the domain of material characterization. Despite the rapid development of different materials including glass and carbon fiber-reinforced polymer–matrix composites, techniques for characterization of their constitutive properties have had limited advance [5]. Conventional measurement techniques are usually employing a resistance strain gauge and extensometer. In fact, the strain measured by a strain gauge or an extensometer is the average strain in a small area/length of an object. Therefore, in order to measure the strain at several points, a number of gages must be installed on the surface which is a cumbersome and expensive task. Full-field-deformation measurement techniques are more flexible than conventional methods for the derivation of stress–strain relations [5]. Various non-contact methods have been developed for full-field strain measurements such as non-interferometric techniques and a number of variant interferometric techniques [6]. The interferometric methods, in addition to a coherent light source isolated in the laboratory condition, require fringe processing and phase analysis techniques to assess the deformation. However, non-interferometric techniques such as DIC techniques, in general, demand simpler requirements under experimental conditions and specimen preparation [6].

The application of the DIC technique for strain assessment in the characterization of nonlinear interlaminar shear stress–strain response of a Short-Beam Shear (SBS) test composed of glass/epoxy tape was a successful experiment [7]. An accurate test method was developed by Yihong et al. [2] for the assessment of nonlinear shear stress–strain relations of thick composite materials using DIC and finite element analysis. Mechanical properties of a hybrid composite under tensile loading were also characterized using a strain gauge and DIC technique [8, 9].

Nevertheless, there are several parameters influencing the accuracy of the strain field computed by the DIC technique which can be categorized into two classes. The first class includes the parameters which are associated with the equipment and setting, such as the quality of speckle patterns [10], light source, resolution of images, and imaging noise [11]. In general, it is recommended to use higher-resolution images to minimize measurement error [12]. Other image features such as noise which causes mean bias error (systematic error) should be considered although this error may be neglected in comparison with standard deviation

*Corresponding author's email: r_sarfaraz@sbu.ac.ir

error (random error) [12]. The quality of the speckle pattern is another parameter influencing the accuracy of strain calculation [10-14]. The surface subjected to analysis must contain some visible contrast between the background and speckle color to recognize its pixels' track easily [14]. The effects of surface painting on the image and pattern quality were investigated by applying different methods for painting the object's surface. Based on this study, it is claimed that the airbrush leads to more accurate results than the spraying method. Moreover, patterns with a white background have a flatter distribution of speckle sizes rather than those with black background [12]. Another research also shows that by increasing the density of speckles in subsets, measurement error and the uniqueness of patterns declined. In other word, as concluded in [15], subsets must contain enough unique and identifiable features to achieve a reliable and accurate displacement determination.

The second class of parameters, called calculation parameters, for instance, the subset size [15-18], speckle size [10, 11], correlation criterion [19, 20], subset shape function [21], and interpolation scheme [21] could affect the accuracy of results during the calculation of strain. Crammond et al. [12] proved that calculation parameters can affect the strain field more than speckle patterns. Throughout the analysis process, the surface of an object is divided into a grid which involves interrogation cells or subsets which contain finite pixels to be analyzed by the DIC technique. The effect of subset size on calculated strain field has been studied based on empirical observations, however, there is no common agreement on the most appropriate setting of subset size to be more practical for various case studies [22]. It can be inferred from these studies that the optimum subset size is the smallest possible subset size which does not lead to noisy strain data and accurately approximates the deformation field using first- and second-order subset shape functions. This conclusion is based on the fact that a larger subset size tends to have a smoothing effect [22]. Besides, it was shown that the accuracy of displacement measured for three different surface paintings with different sizes of speckle patterns increased when subset sizes increased although for the same subset sizes surface patterns with larger visible image contrast provides more accurate results [15]. However, increasing the subset size results in lower computational performance due to the time required for the solution of respective equations, and therefore the subset size should have an upper limit. The compromise between subset size, accuracy, noise, and computational efficiency is more difficult for nonhomogeneous displacement fields that both lower and limits exist for the subset size [18].

In spite of the fact that the aforementioned parameters significantly affect the outputs of the DIC technique, existing studies do not provide straightforward recommendations for the optimum setup of the DIC parameters, and a trial-and-error process is usually required. In the current study, the influence of these parameters on the accuracy of strain field measurement is investigated in the context of material characterization application. An open-source 2-D DIC program, known as Ncorr and developed at the Georgia Institute of Technology, was employed for the analyses. In addition to the speckle size, called the Region Of Interest (ROI) in this program, two parameters known as subset spacing and subset radius size in this program are also studied. As the speckle pattern quality, namely the speckle pattern entropy and identifiable features in a definite subset radius can also affect the accuracy of the measured strain field, the sizes of the speckle pattern are intentionally changed. The tensile elastic modulus of carbon/epoxy specimens is calculated by using the DIC technique and the results are compared with the measurements of a conventional extensometer. In addition to the accuracy of measurements, the influence of alteration in these parameters on the required processing time is also assessed. The present study is aimed to propose explicit recommendations regarding the optimum setting of DIC parameters, based on the experimental results, in order to minimize the processing time while reducing the sensitivity to the selection of parameters.

2- Experimental Program

The material characterization is conducted on a unidirectional composite laminate constituent of the low-temperature cure carbon/epoxy prepreg SE70 lamina from Gurit ST™ with a nominal thickness of 0.2 mm for each layer. The laminate composed of ten layers of prepreg lamina was fabricated by the vacuum bag method. The lay-ups were cured for about 12 hours at 78°C under vacuum with a heating/cooling rate of nearly 0.5 °C/min. The cured laminates with approximately 2 mm thickness were cut to create totally five specimens in the transverse direction with an overall length of 175 mm. The detailed dimensions of the specimens are presented in Table 1.

The specimens were painted white as the background color followed by a black spray to create visible and distinguishable features on the surface as shown in Fig. 1 As has been stated in Ref. [12], airbrush provides better results than spraying, however, when a white color is chosen as the background, the differences between airbrush and spraying is marginally decreased.

An image processing script was employed to characterize the speckle patterns. The average feature size and the corresponding standard deviation calculated for each specimen are presented in Table 1. A representative statistical distribution of feature size is also shown in Fig. 2

The experiments were performed following the standard ASTM D3039-08 [23]. The specimens were loaded in uniaxial tension using an MTS hydraulic testing machine under a cross-head speed of 2 mm/min. The applied load and displacement were continuously recorded by a 100 kN load cell and the cross-head position respectively. The strain along the loading direction was also measured using a 634.25 MTS axial extensometer. A high-resolution CCD camera connected to a computer was used to capture 12-bit, 1392×1040 pixel digital images of the speckle pattern painted on the specimens (see Fig. 1). Details of the image acquisition system and all settings employed for the DIC analysis are provided in Tables 2 and 3.

Table 1. Dimensions of specimens and characteristics of speckle patterns and measured modulus of elasticity by the extensometer

Specimen ID.	Width (mm)	Thickness (mm)	Speckle pattern		Modulus of elasticity (GPa)	
			Average feature size (micron)	Standard deviation (micron)	Secant Method	Curve fitting method
T1	20.40±0.06	2.06± 0.00	620	346	7.1495	7.1462
T2	20.60±0.02	2.03± 0.01	521	263	7.3685	7.3724
T3	20.00±0.05	2.02± 0.00	448	210	7.4294	7.4354
T4	20.10±0.02	2.03± 0.00	527	270	7.2228	7.2242
T5	20.10±0.04	2.04± 0.00	529	260	7.3162	7.3131

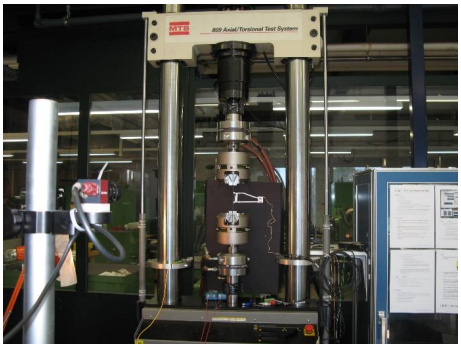

(a)

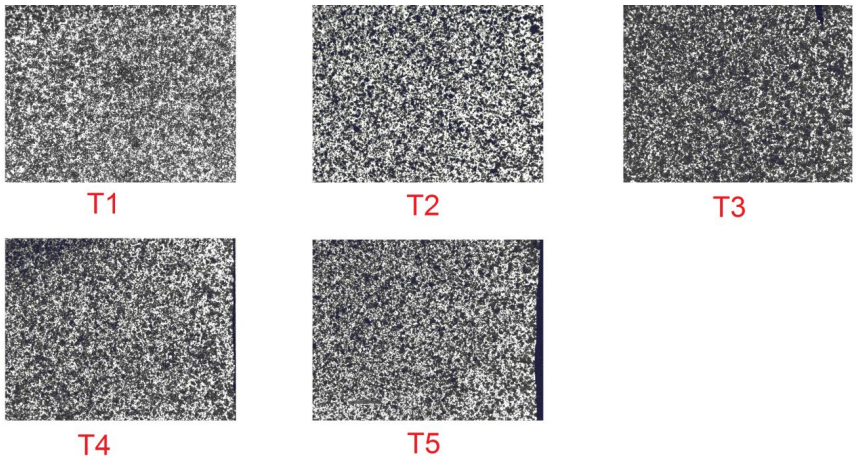

(b)

Fig. 1. (a) Experimental setup and (b) illustrations of speckle pattern on the surface of specimens.

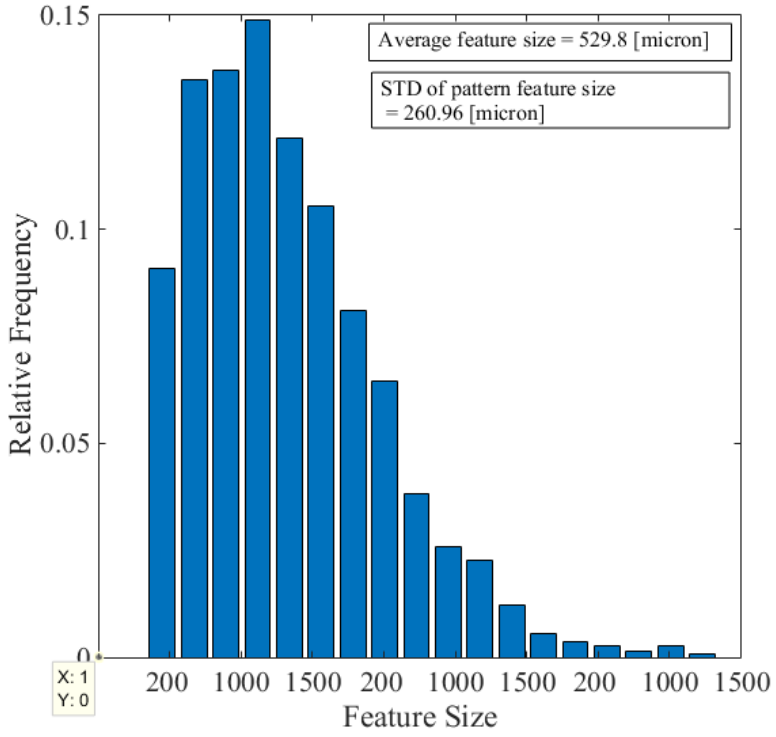

Fig. 2. Statistical distribution of pattern feature size for specimen T5

Table 2. Details of the image acquisition system

CCD Camera	Guppy F-146B camera 12bit
Resolution	1392×1040
Cell size	4.65 µ
Lens	Cosmicar TV lens 1.4/25 mm
Lens Aperture	f/8
Field-of-View (FOV)	25×20 mm×mm
Stereo-Angle	Single camera with straight imaging
Pattern Technique	Using black spray to make speckled pattern on the white background
Stand-off Distance	80 cm
Image Acquisition Rate	1 Hz

Table 3. Details of the DIC analysis system and corresponding parameter settings

DIC Software	Georgia Institute of Technology, Ncorr, Version 1.2 .2.
Image Filtering	Not used
Subset Radius	Changing from 10 to 60 pixels for this study
Subset Spacing	Changing from 2 to 10 pixels for this study
Matching Correlation Criteria	Normalized Cross Correlation (NCC)
Interpolant	Bi-quintic B-splines
Strain Formulation	Green-Lagrangian

3- Selected Parameters Influencing the Performance of the DIC Technique

Three parameters influencing the outputs of DIC analysis are investigated in the following, i.e. region of interest, subset size, and subset spacing. This terminology refers to the convention defined in the Ncorr program and may be denoted with different terms in various programs and references. Therefore, the definition of these terms and their admitted influence on the DIC results are briefly explained.

3- 1- Region of interest

Region of Interest (ROI) is a subdivision of an image being processed by the DIC technique and its size can be from a few pixels up to the whole image. Commonly, in many commercial programs, this region is primarily delimited by the user at the beginning of the correlation procedure and introduced to the DIC program. Increasing the size of ROI demands extra computational resources while by decreasing its size, much information may be lost or it may lead to a wrong analysis [24].

In order to study the influence of ROI size on the analysis, three different sizes are examined; 12.5%, 25%, and 50% of the area of whole images in a squared-shaped form located at the center of images as presented in Fig. 3 In this part of the study, the subset spacing takes the values of 2, 6, and 10 pixels and subset radiuses are 12, 24, 36, 48, and 60 pixels. On the basis of these results, the most appropriate size of ROI is determined and the rest of the parametric studies are carried out based on the selected size.

3- 2- Subset Radius

When the ROI is introduced into the program in the subset-based DIC programs such as Ncorr, this region must be divided into smaller areas which are called subsets. Subsets, in the Ncorr program, are initially defined as a group of adjacent areas in a circular form that includes integer pixel locations in the reference image [25]. The radius of these circles, as shown in Fig. 4, is called subset radius (SR) and is the same for all subsets in an analysis. As it has been mentioned in the manual of the software, appropriate sizing of the subset radius is the main component of DIC analysis which has to be optimized iteratively using a heuristic process due to its influence on the performance of the analysis [22]. The subset radius size which is studied in the following sections varies in the range of 10 to 60 pixels with a step size of 10 leading to in total of six different subset radiuses.

3- 3- Subset spacing

Subset spacing (SS) is a calculation parameter that determines the distance between two consecutive subsets in the region of interest. As it is shown in Fig. 5, the highlighted dots represent the location of subsets centers. Therefore, by decreasing the subset spacing, the number of subsets that must be analyzed is increased. According to reviewed literature, small subset spacing enhances the quality and accuracy of outputs while the processing time is significantly increased. The subset spacing in Ncorr program can range from 0 to 10. In the current study, the subset spacing of 2, 3, 4, 6, 8, and 10 pixels are studied. Therefore, a total of 36 cases are studied in combination with various subset radius sizes and compared with experimental data recorded by the extensometer. For more clarity, a unified label is defined for all case studies as SSx-SRy where SS and SR stand for subset spacing and subset radius respectively, and x/y represents their corresponding values.

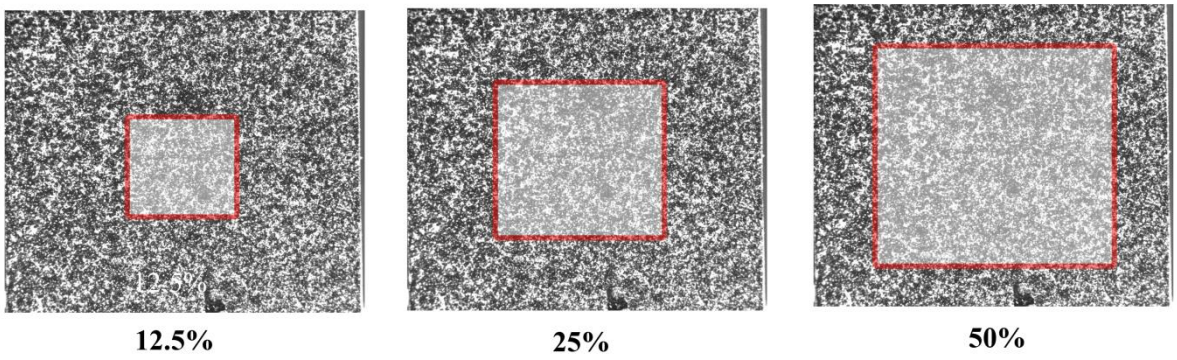

Fig. 3. Representation of three different sizes of ROI regarded on images.

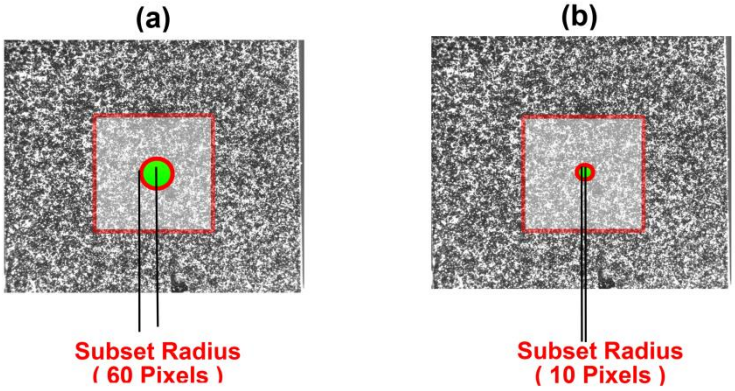

Fig. 4. Representation of two different subset radiuses (a) SR=60 and (b) SR=10 in a reference image

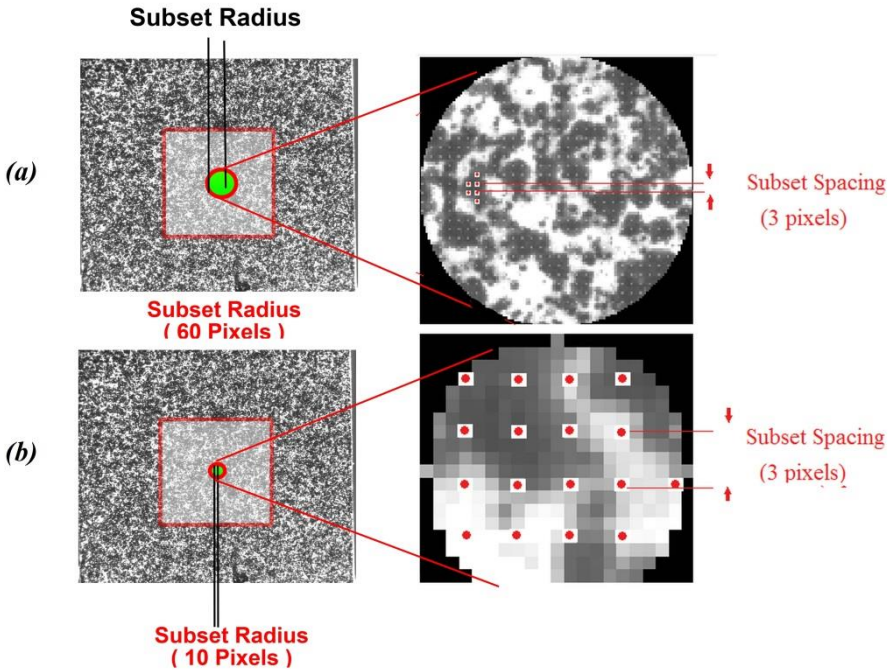

Fig. 5. Illustration of (a) subset spacing of 3 pixels and subset radius of 60 pixels and (b) subset spacing of 3 pixels and subset radius of 10 pixels

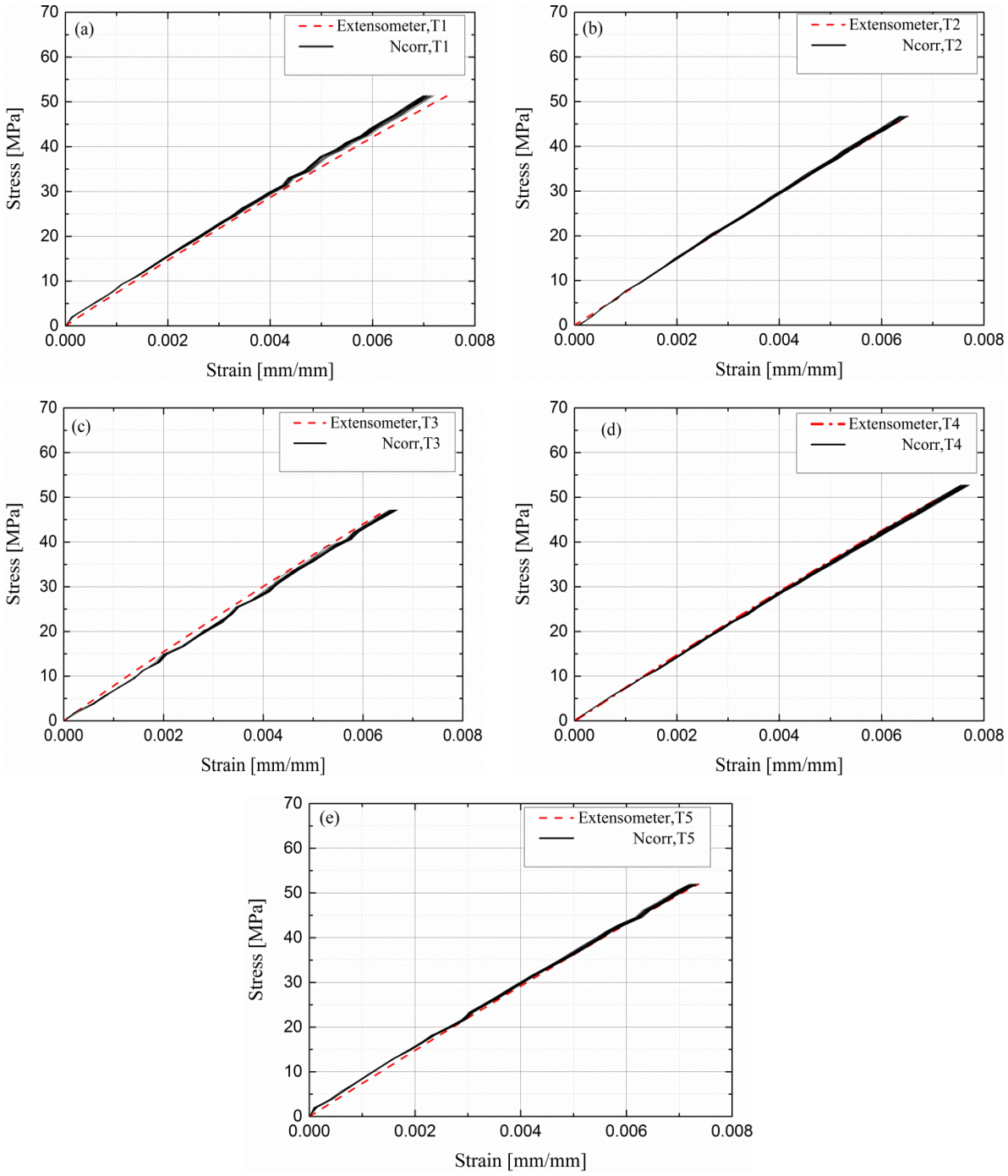

Fig. 6. Comparison of stress-strain curves acquired by DIC analysis (including 36 curves in each graph by applying different parameters setting) and extensometer for specimens (a) T1, (b) T2, (c) T3, (d) T4, and (e) T5.

4- Results and Discussion

The stress-strain curves derived by variation of DIC parameters are compared with the extensometer results in Fig. 6 for specimens T1 to T5. The DIC results, including 36 curves in each graph, are clustered in a small width band with few notable features. Apparently, in all specimens, this bandwidth is widened as the stress level is increased. Also, the DIC curves are not as smooth as the curves acquired by the extensometer. The roughness of curves varies between the specimens with the smoothest one presented by specimen T2. In general, a moderate deviation can be recognized between the DIC results and the extensometer measurements except for specimen T2 where a fairly well accordance can be observed. In order to quantify the error introduced by applying different settings for the DIC analysis, an error index is defined by Eq. (1),

$$Error\ index = \frac{\sum_{i=1}^{n} \left| \varepsilon_{i,Ncorr} - \varepsilon_{i,Extensometer} \right|}{n} \quad (1)$$

where $\varepsilon_{i,Ncorr}$ and $\varepsilon_{i,Extensometer}$ are the strains calculated by the DIC and the strains measured by the extensometer respectively and n is the number of images. In the current study, an equal number of images are employed for the analyses.

4- 1- Influence of region of interest

The effect of ROI size on the outputs of DIC analysis is examined for two representative specimens T1 and T2 which visually demonstrate erroneous and accurate cases respectively. Error indices are calculated using Eq. (1) for all combinations of subset spacing (2, 6, and 10 pixels), subset radius (12, 24, 36, 48, and 60 pixels), and ROI of 12.5%, 25%, and 50% of the image size. In order to examine the influence of each parameter on the variation of error-index, for both specimens, the Standard Deviations (STD) of computed error indices for fixed values of SS and SR are calculated and plotted in Fig. 7 Apparently, the results corresponding to the ROI size of 12.5% systematically display the highest STDs independent of the size of SS and SR. In contrast, the curves related to the highest ROI size present the least variation and much better consistency among the results calculated at different settings for SS and SR. Therefore, regardless of the overall accuracy of the results, increasing the ROI size reduces the sensitivity of the DIC analysis to the variation of SS and SR. Therefore, the largest ROI size, which is 50% of the image size, is selected as the reference size for the subsequent analyses, aware of its time penalty.

4- 2- Influence of subset radius

The influence of subset radius on the induced error is studied from two aspects i.e. the strain calculation error and the error induced in the determination of "modulus of elasticity" as one of the most important parameters in the material characterization domain. The results and discussions regarding these aspects are detailed in the following two subsections.

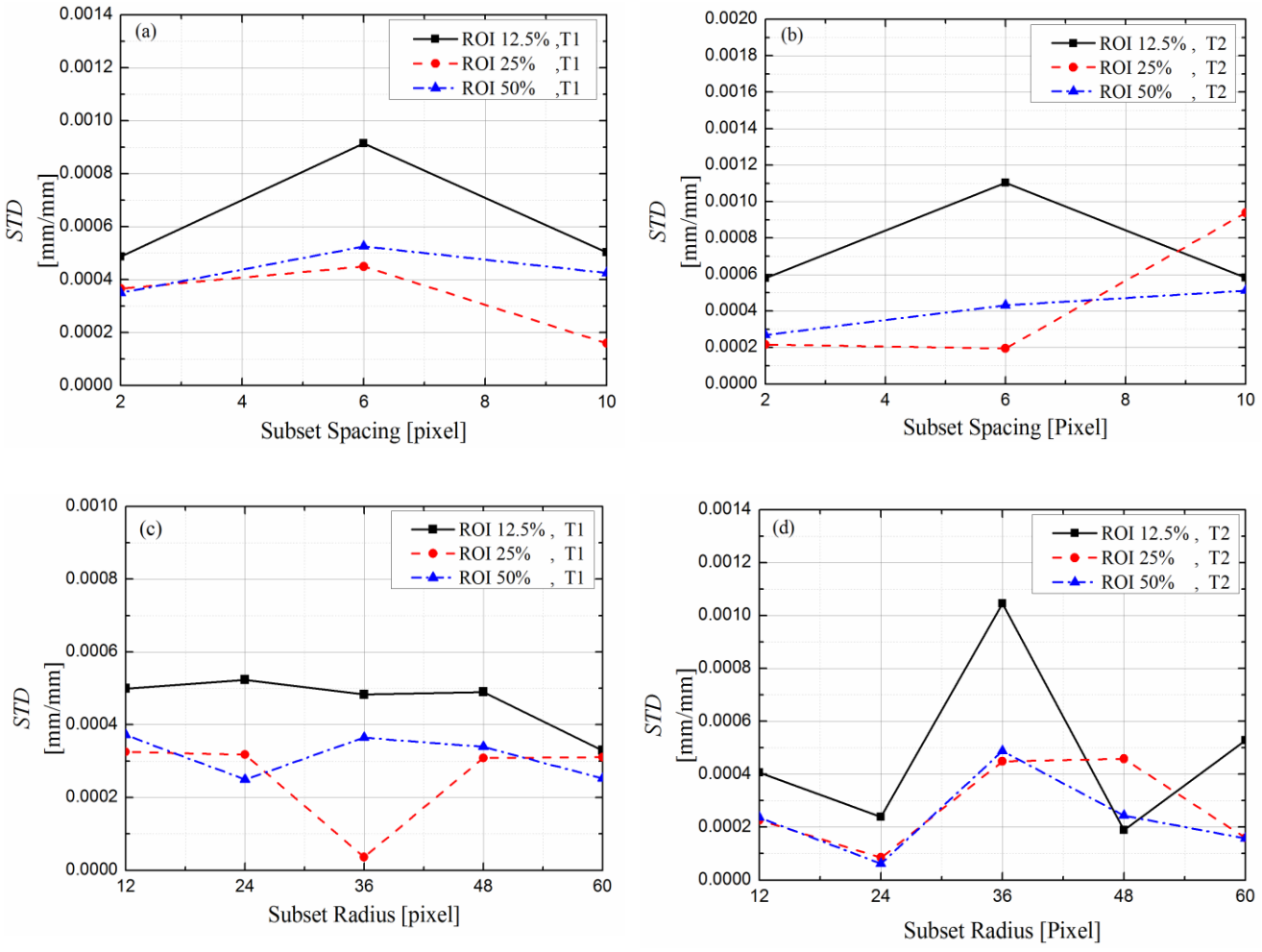

Fig. 7. Variation of STD in terms of (a) subset spacing for specimen T1 (b) subset spacing for specimen T2 (c) subset radius for specimen T1 and (d) subset radius for specimen T2.

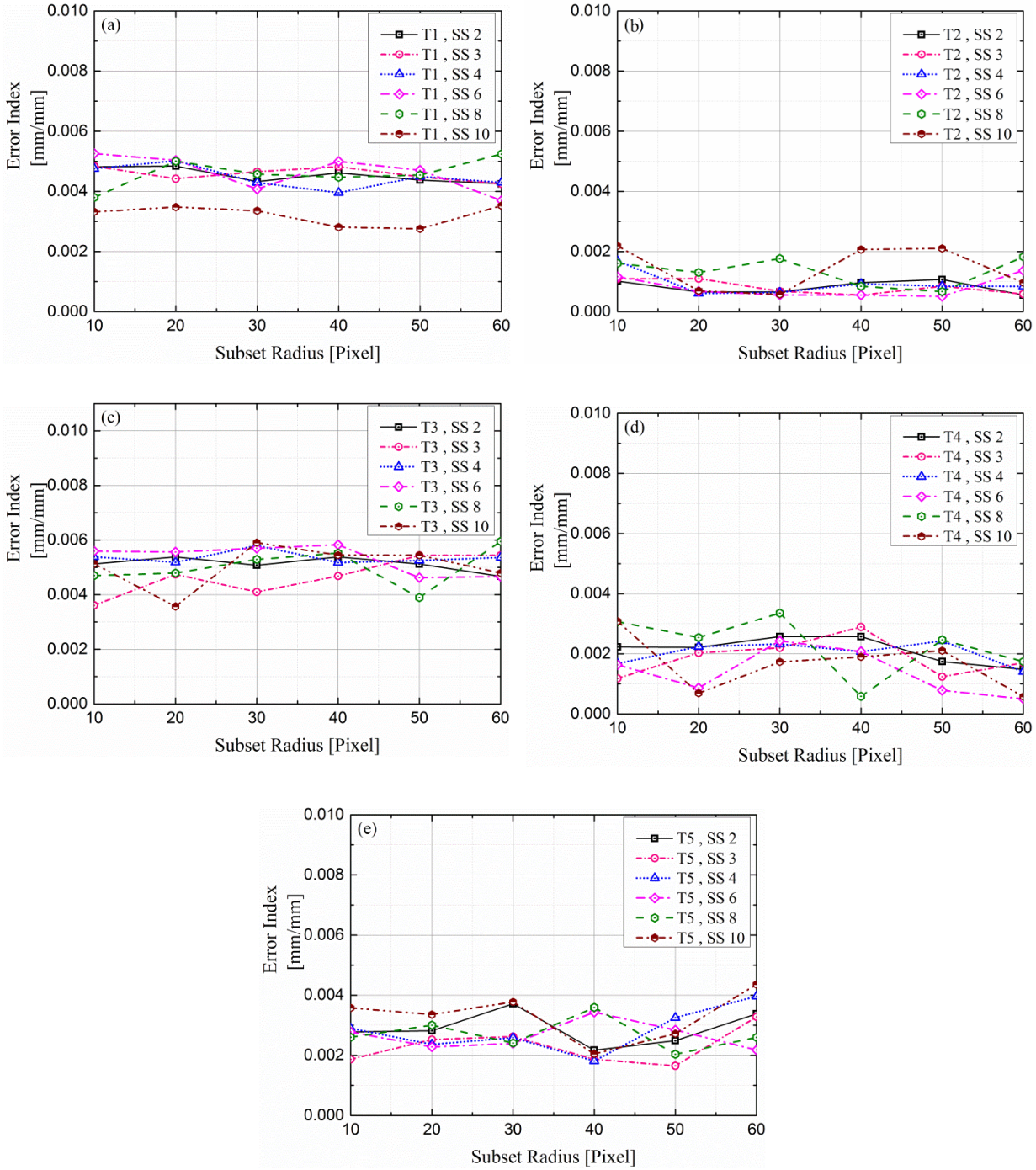

Fig. 8. Variation of error index at different SSs in terms of SR for specimens (a) T1, (b) T2, (c) T3, (d) T4, and (e) T5.

4- 2- 1- Influence on the strain error

Variations of error indices in terms of SR at constant values of SSs are shown in Fig. 8 for all specimens. The curves do not present any specific trend except that the level of error independent of the size of SS and SR is different between specimens; being the highest for T1 and T3 and the lowest for T2, consistent with the curves presented in Fig. 6 Therefore, considering the growth of computation time required for analysis with small SSs, choosing of a large SS would improve the efficiency of the DIC analysis.

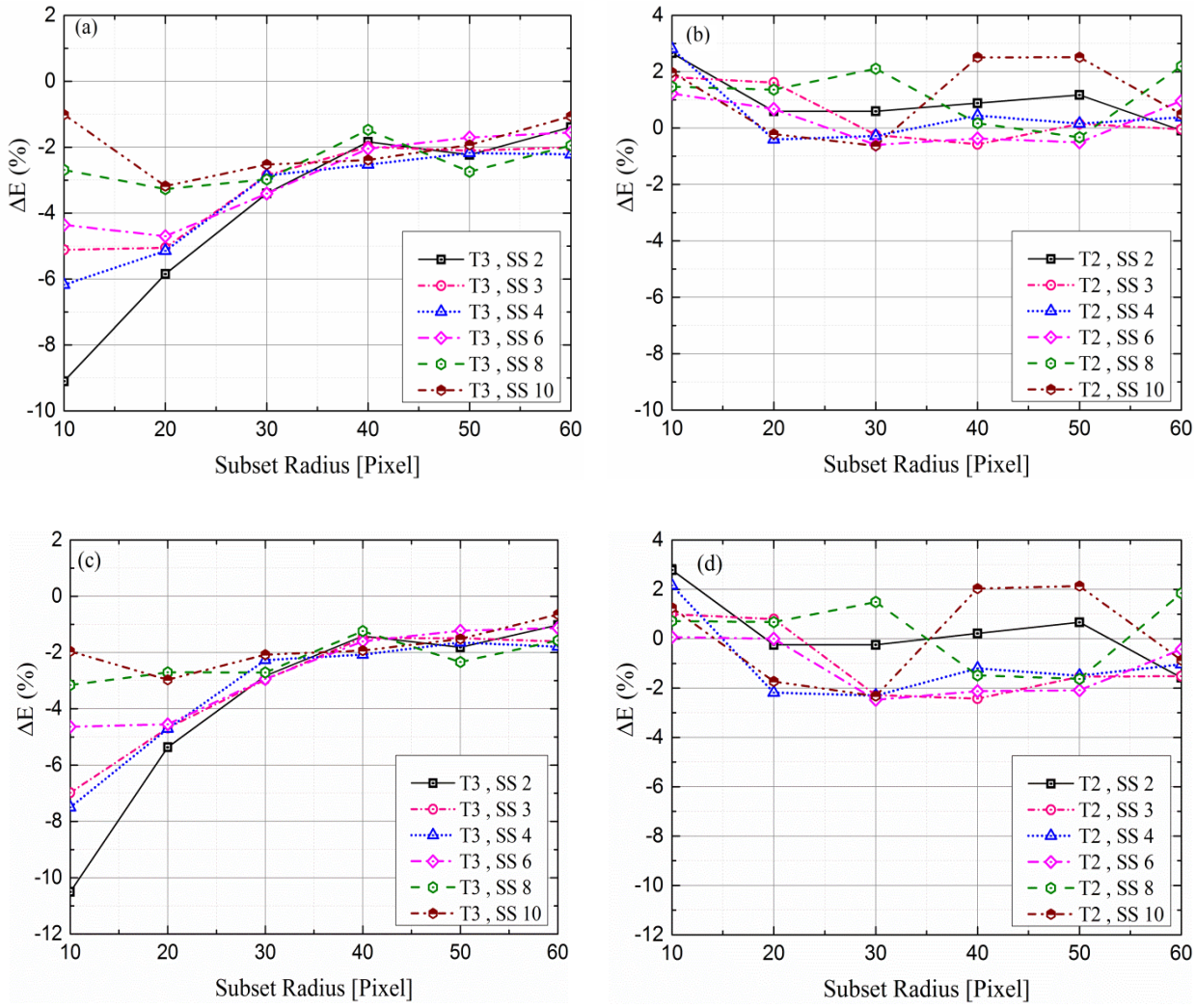

Fig. 9. Variation of error in calculated modulus of elasticity at different SSs in terms of SR for the specimen (a) T3 using fitting method (b) T2 using fitting method (c) T3 using secant method (d) T2 using secant method.

4- 2- 2- Influence on the modulus of elasticity

The modulus of elasticity is calculated for specimens T2 and T3 representatives of the best and worst cases based on two methods; i.e. the fitting method (the slope of a line fitted to the entire range of the stress-strain data) and the secant method (the slope of the line passing through the points corresponding to 1000 and 3000 μmm/mm strain). Minimum and maximum of calculated modulus of elasticity corresponding to different subset radiuses are given in Table 4. The percentage of difference between the moduli calculated from DIC analysis and the extensometer, ΔE, computed for these specimens are presented in Fig. 9

An apparent difference between the curves is observed in Figs. 9a and 9c corresponding to specimen T3. The difference among the curves representing various SSs is higher at small SRs and it is diminished as the SR is increased. The error can reach approximately 9% using the fitting method (Fig. 9a) and more than 10% employing the secant method (Fig. 9c) However, in specimen T2, without any common trend, the error level remains less than 3% for any alteration in parameters. Therefore, it can be inferred that enlarging the SR suppresses the sensitivity of the analysis to the variation of SS although this tip demands more computational time. The significance of this conclusion is particularly highlighted when the user is not aware of the quality of the speckle pattern and other parameters that may affect the results and make the analysis insensitive to these variables.

4- 3- Influence of subset spacing

Similar to the study carried out for the influence of SR, in the following subsections, the effect of SS on the error related to the calculation of strains and the error induced in the determination of modulus of elasticity are investigated.

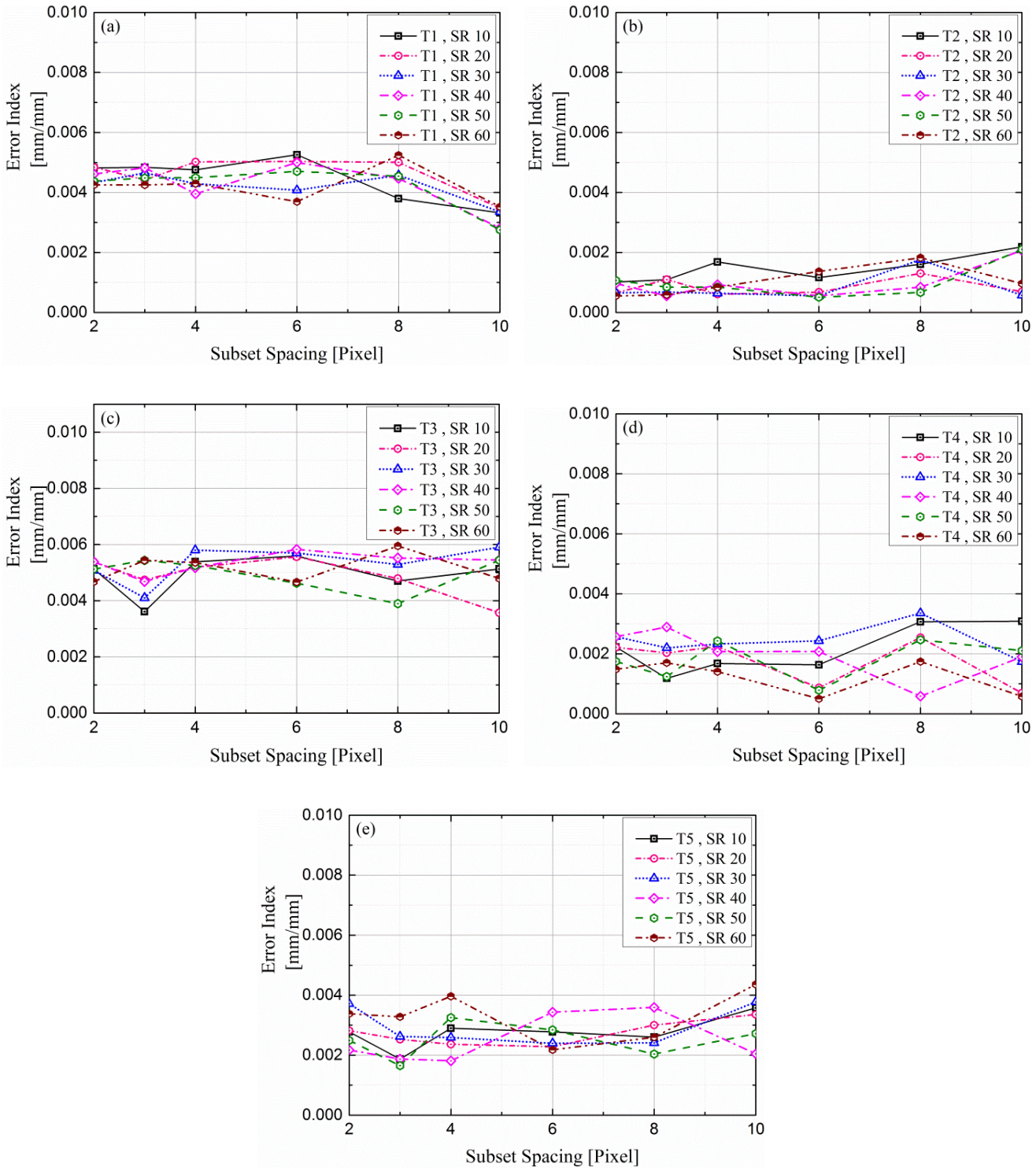

Fig. 10. Variation of error index at different SRs in terms of SS for specimens (a) T1, (b) T2, (c) T3, (d) T4, and (e) T5.

4- 3- 1- Influence on strain error

Variations of error indices with respect to SS at different SRs are presented in Fig.10 In all specimens, the difference between the error indices at and small values of SS, particularly at SS=2 pixels, is trivial. However, the difference is slightly amplified as the subset spacing is increased and more dependency on the size of SR is observed. Moreover, variation of the SR would not result in any specific change in the error-index, although choosing a smaller SR would reduce the computational time.

Table 4. Minimum and maximum calculated modulus of elasticity corresponding to different subset radiuses (units in GPa)

Figure No.	*SR10*		*SR20*		*SR30*		*SR40*		*SR50*		*SR60*	
	Min	Max	Min	Max	Min	Max	Min	Max	Min	Max	Min	Max
Fig. 9a	6.74	7.34	6.98	7.18	7.16	7.23	6.98	7.31	6.99	7.29	7.25	7.34
Fig. 9b	7.48	7.58	7.34	7.50	7.33	7.53	7.33	7.56	7.33	7.56	7.37	7.53
Fig. 9c	6.65	7.28	7.03	7.23	7.21	7.27	7.25	7.34	7.26	7.34	7.30	7.39
Fig. 9d	7.37	7.57	7.21	7.43	7.19	7.48	7.19	7.52	7.22	7.53	7.25	7.50

4- 3- 2- Influence on the modulus of elasticity

Both methods for computation of modulus of elasticity are applied to specimens T2 and T3 to examine the effect of SS on the analysis error. The minimum and maximum calculated modulus of elasticity corresponding to different subset spacings are given in Table 5. The calculated errors for specimen T3 as presented in Figs. 11a and 11c show that at small SS, the error calculated by both methods is relatively high especially for small SR, reaching approximately 10%. However, the sensitivity to SS size is significantly decreased as the SR is enlarged. This argument is not applied to the results acquired for specimen T2 where the overall error is as low as 3% and no regular trend is observed between different settings of parameters. Therefore, it can be recognized that adjusting the SR to a large value reduces the sensitivity of the outputs to the SS size which is a very important factor especially when the quality of the image and the speckle pattern is susceptible.

4- 4- Influence on computation time

The computation time for DIC analysis is recorded for all analyses as presented in Fig. 12 the decrease of subset spacing significantly results in an increase in the computation time. As well, the required processing time, almost linearly, increases as the SR is enlarged. Therefore, keeping SS and SR at their highest values enables the most efficient analysis in terms of time, while suppressing any influence from poor speckle patterns contributing to the calculation error. However, it can be noticed from the presented trends in the figures that the influence of SS size on the computation time is magnified at large SR sizes, for instance, the decrease of SS size from 10 to 2 at SR=60 leads to approximately 12 times increase in the computation time while at small SRs the size of SS does not play an important role in the processing time.

5- Conclusions

The performance of a typical DIC analysis for the derivation of strain field and measurement of material properties of a composite laminate subjected to monotonic loading was assessed by comparing its results with data recorded by a conventional extensometer. The influence of a couple of DIC setting parameters on the accuracy of analysis was studied. The following conclusions can be drawn from this investigation,

The increase in ROI size reduces the sensitivity of the analysis to the setting parameters although it demands more computational resources. The calculated errors in the strain field corresponding to analyses with the largest ROI size exhibit the least variation with respect to the changes in subset radius and subset spacing.

Enlarging the subset radius may not affect the overall strain error, however, it diminishes the sensitivity of the computed modulus of elasticity to the subset spacing. Also, the increase in subset spacing leads to a minor increase in error which is usually obscured by other errors.

Enlarging the SR and decrease of SS result in the increase of required processing time. However, compromising the time cost and accuracy while having the minimum sensitivity to the DIC parameters and image quality, adjusting large SRs and SSs are recommended for a typical DIC analysis in order to determine the material properties at low strain rates.

Ethical statement

The authors of this article state that the research has been conducted according to ethical standards.

Conflict of interest

The authors declare that they have no conflict of interest.

Acknowledgment

The authors would like to express their gratitude to Prof. John Botsis, head of the LMAF laboratory at Ecole Polytechnique Fédérale de Lausanne (EPFL), for his kind support in performing the experimental program.

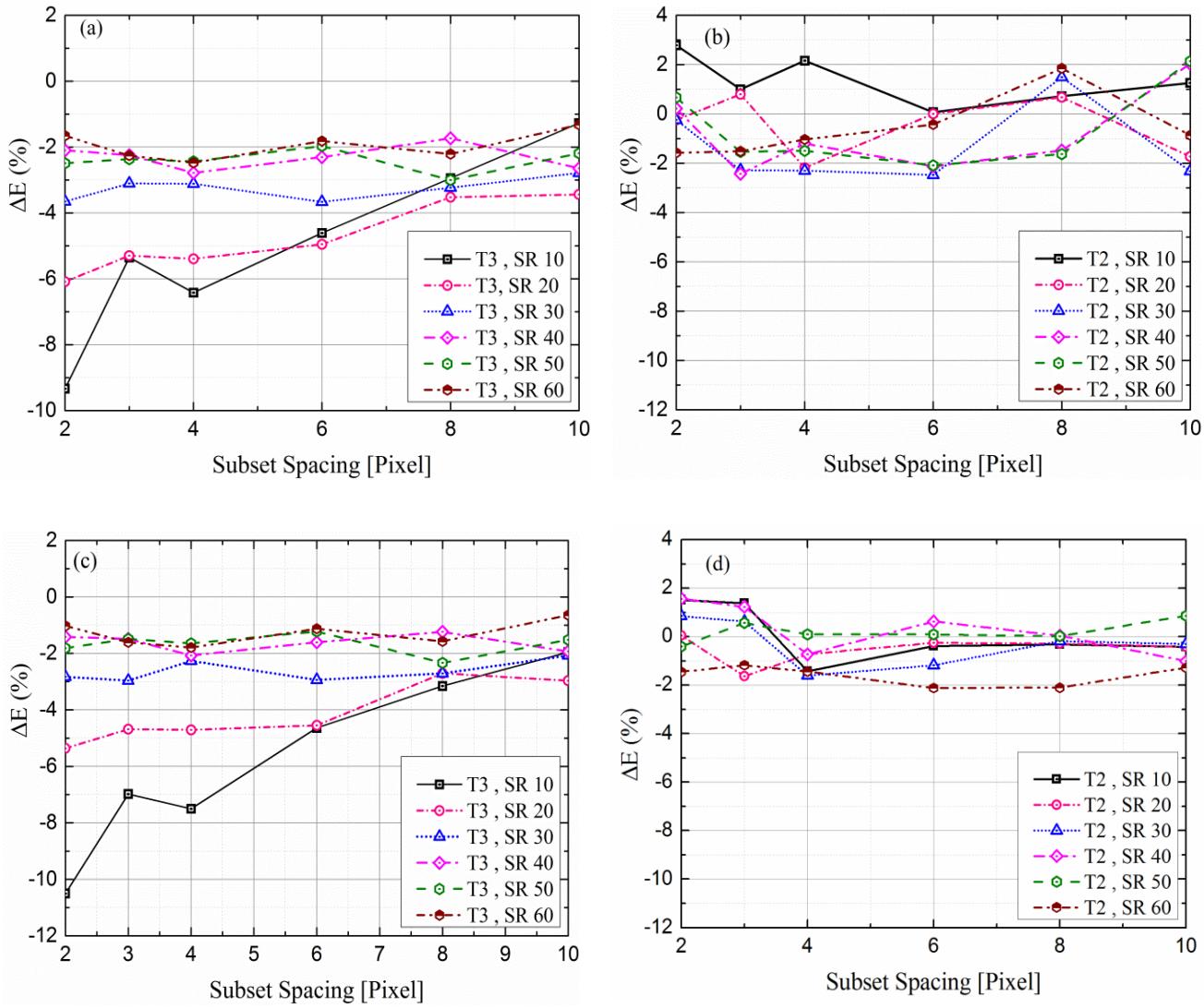

Fig. 11. Variation of error in calculated modulus of elasticity at different SRs in terms of SS for the specimen (a) T3 using fitting method (b) T2 using fitting method (c) T3 using secant method (d) T2 using secant method.

Table 5. Minimum and maximum calculated modulus of elasticity corresponding to different subset spacings (units in GPa)

Figure No.	*SS 2*		*SS 3*		*SS 4*		*SS 6*		*SS 8*		*SS 10*	
	Min	Max	Min	Max	Min	Max	Min	Max	Min	Max	Min	Max
Fig. 11a	6.74	7.31	7.03	7.27	6.96	7.25	7.07	7.30	7.17	7.27	7.18	7.34
Fig. 11b	7.37	7.57	7.33	7.50	7.34	7.58	7.33	7.46	7.38	7.53	7.33	7.52
Fig. 11c	6.65	7.35	6.91	7.32	6.87	7.31	7.08	7.35	7.19	7.34	7.21	7.38
Fig. 11d	7.25	7.57	7.19	7.44	7.20	7.53	7.19	7.37	7.26	7.50	7.20	7.53

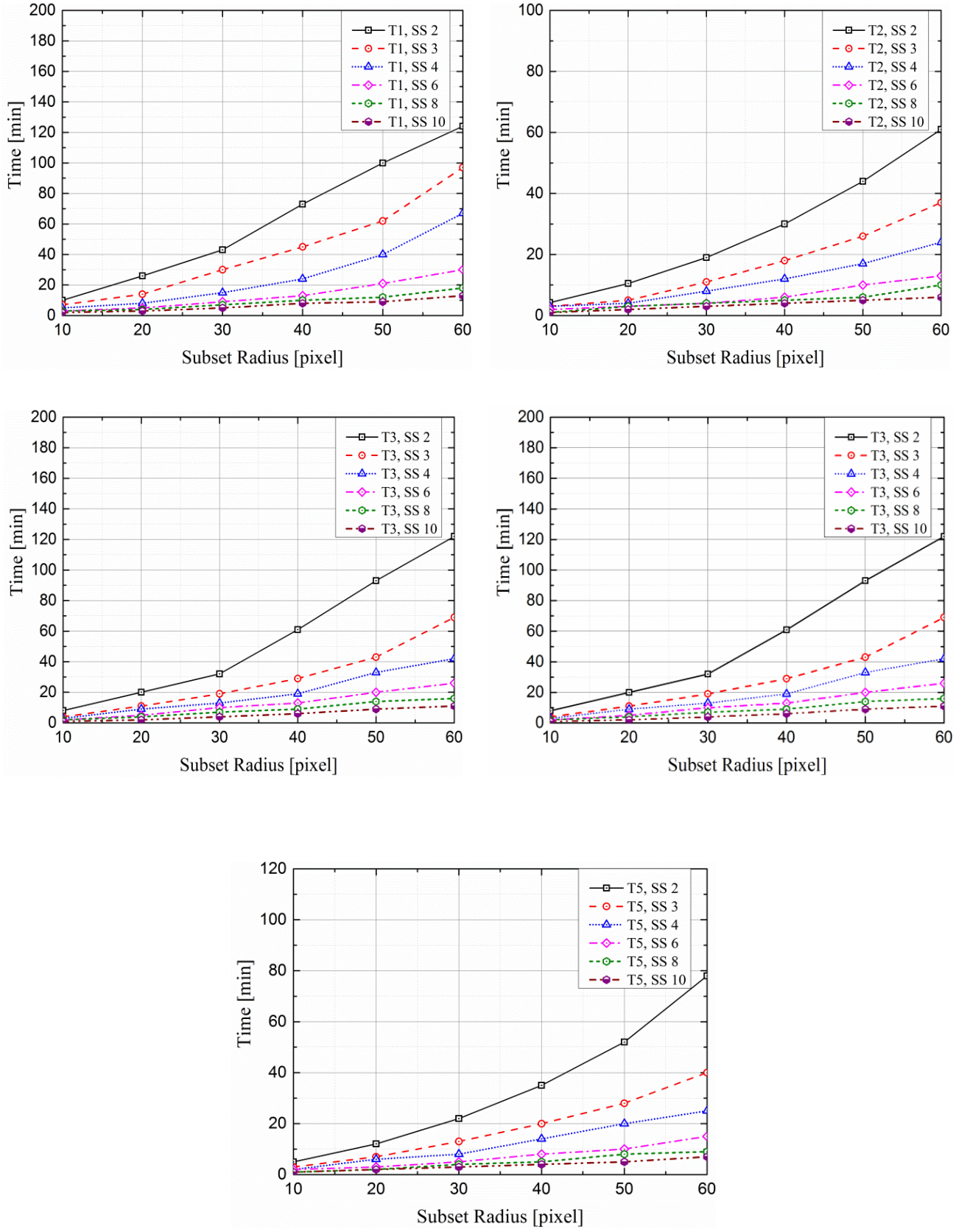

Fig. 12. Computation time recorded for DIC analysis at different parameter settings for specimens (a) T1, (b) T2, (c) T3, (d) T4, and (e) T5.

References

[1] P. Corigliano, V. Crupi, E. Guglielmino, Non linear finite element simulation of explosive welded joints of dissimilar metals for shipbuilding applications, Ocean Engineering, 160 (2018) 346-353.

[2] Y. He, A. Makeev, B. Shonkwiler, Characterization of nonlinear shear properties for composite materials using digital image correlation and finite element analysis, Composites Science and Technology, 73 (2012) 64-71.

[3] S. Bhattacharjee, D. Deb, Automatic detection and classification of damage zone (s) for incorporating in digital image correlation technique, Optics and Lasers in Engineering, 82 (2016) 14-21.

[4] X. Chen, Z. Yu, H. Wang, C. Bil, Strain monitoring on damaged composite laminates using digital image correlation, Procedia Engineering, 99 (2015) 353-360.

[5] A. Makeev, Y. He, P. Carpentier, B. Shonkwiler, A method for measurement of multiple constitutive properties for composite materials, Composites Part A: Applied Science and Manufacturing, 43(12) (2012) 2199-2210.

[6] B. Pan, K. Qian, H. Xie, A. Asundi, Two-dimensional digital image correlation for in-plane displacement and strain measurement: a review, Measurement science and technology, 20(6) (2009) 062001.

[7] A. Makeev, C. Ignatius, Y. He, B. Shonkwiler, A test method for assessment of shear properties of thick composites, Journal of composite materials, 43(25) (2009) 3091-3105.

[8] A.F. Ab Ghani, J. Mahmud, Material Characterization of Hybrid Composite: Experimental Using Strain Gauge/ DIC with Finite Element Modelling Macro/Micro Scale, Key Engineering Materials, 740 (2017) 31 - 40.

[9] M.C. Isa, A.R.A. Manaf, M.H. Anuar, A.F. Ab Ghani, J. Mahmud, S. Nazran, N. Muhammad, R.M. Amman, S.D. Malingam, I. Abu-Shah, SCIENCE & TECHNOLOGY RESEARCH INSTITUTE FOR DEFENCE (STRIDE), Development, 240 (2018) 246.

[10] B. Pan, Z. Lu, H. Xie, Mean intensity gradient: an effective global parameter for quality assessment of the speckle patterns used in digital image correlation, Optics and Lasers in Engineering, 48(4) (2010) 469-477.

[11] Y. Wang, M. Sutton, H. Bruck, H. Schreier, Quantitative error assessment in pattern matching: effects of intensity pattern noise, interpolation, strain and image contrast on motion measurements, Strain, 45(2) (2009) 160-178.

[12] G. Crammond, S. Boyd, J. Dulieu-Barton, Speckle pattern quality assessment for digital image correlation, Optics and Lasers in Engineering, 51(12) (2013) 1368-1378.

[13] B. Pan, B. Wang, G. Lubineau, Comparison of subset-based local and FE-based global digital image correlation: Theoretical error analysis and validation, Optics and Lasers in Engineering, 82 (2016) 148-158.

[14] T. Hua, H. Xie, S. Wang, Z. Hu, P. Chen, Q. Zhang, Evaluation of the quality of a speckle pattern in the digital image correlation method by mean subset fluctuation, Optics & Laser Technology, 43(1) (2011) 9-13.

[15] B. Pan, H. Xie, Z. Wang, K. Qian, Z. Wang, Study on subset size selection in digital image correlation for speckle patterns, Optics express, 16(10) (2008) 7037-7048.

[16] D. Lecompte, A. Smits, S. Bossuyt, H. Sol, J. Vantomme, D. Van Hemelrijck, A. Habraken, Quality assessment of speckle patterns for digital image correlation, Optics and lasers in Engineering, 44(11) (2006) 1132-1145.

[17] H. Haddadi, S. Belhabib, Use of rigid-body motion for the investigation and estimation of the measurement errors related to digital image correlation technique, Optics and Lasers in Engineering, 46(2) (2008) 185-196.

[18] S. Yaofeng, J.H. Pang, Study of optimal subset size in digital image correlation of speckle pattern images, Optics and lasers in engineering, 45(9) (2007) 967-974.

[19] W. Tong, An evaluation of digital image correlation criteria for strain mapping applications, Strain, 41(4) (2005) 167-175.

[20] B. Pan, A. Asundi, H. Xie, J. Gao, Digital image correlation using iterative least squares and pointwise least squares for displacement field and strain field measurements, Optics and Lasers in Engineering, 47(7-8) (2009) 865-874.

[21] H.W. Schreier, M.A. Sutton, Systematic errors in digital image correlation due to undermatched subset shape functions, Experimental Mechanics, 42(3) (2002) 303-310.

[22] Ncorr V1.2, in: http://www.ncorr.com/download/ncorrmanual_v1_2_2.pdf.

[23] ASTM D3039/D3039M-08,Standard Test Method for Tensile Properties of Polymer Matrix Composite Materials, in, ASTM Internation, West Conshohocken,PA, 2014, pp. 13.

[24] B. Pan, J. Yuan, Y. Xia, Strain field denoising for digital image correlation using a regularized cost-function, Optics and Lasers in Engineering, 65 (2015) 9-17.

[25] J. Blaber, B. Adair, A. Antoniou, Ncorr: open-source 2D digital image correlation matlab software, Experimental Mechanics, 55(6) (2015) 1105-1122.

HOW TO CITE THIS ARTICLE

A. Zarei Aziz, R. Sarfaraz, Influencing Parameters on Tensile Modulus Characterization of Unidirectional Composite Laminates Using Digital Image Correlation Technique, AUT J. Mech Eng., 6(4) (2022) 545-560.

DOI: 10.22060/ajme.2022.20714.6015